

Energy & Environmental Science

Accepted Manuscript



This article can be cited before page numbers have been issued, to do this please use: A. Fuente Cuesta, C. Jiang, A. Arenillas and J. T.S. Irvine, *Energy Environ. Sci.*, 2016, DOI: 10.1039/C6EE01461E.



This is an *Accepted Manuscript*, which has been through the Royal Society of Chemistry peer review process and has been accepted for publication.

Accepted Manuscripts are published online shortly after acceptance, before technical editing, formatting and proof reading. Using this free service, authors can make their results available to the community, in citable form, before we publish the edited article. We will replace this *Accepted Manuscript* with the edited and formatted *Advance Article* as soon as it is available.

You can find more information about *Accepted Manuscripts* in the [Information for Authors](#).

Please note that technical editing may introduce minor changes to the text and/or graphics, which may alter content. The journal's standard [Terms & Conditions](#) and the [Ethical guidelines](#) still apply. In no event shall the Royal Society of Chemistry be held responsible for any errors or omissions in this *Accepted Manuscript* or any consequences arising from the use of any information it contains.



Energy and Environmental Science

PAPER

ROLE OF COAL CHARACTERISTICS IN THE ELECTROCHEMICAL BEHAVIOUR OF HYBRID DIRECT CARBON FUEL CELLS

A. Fuente-Cuesta^a, Cairong Jiang^a, Ana Arenillas^b, John T. S. Irvine^{a†}

There is a growing interest in Hybrid Direct Carbon Fuel Cells (HDCFCs) now considered as one of the most efficient options for the generation of clean energy from mineral coals. In this work, two different hard coals (bituminous and anthracite) have been modified via carbonisation and oxidation and their electrochemical behaviour has been compared in an electrolyte supported HDCFC. A new insight into the HDCFC reaction mechanism is presented, providing an exhaustive analysis taking into account not only the evolution of the properties of the coals upon treatment but also other relevant parameters such as the effect of the cell preparation step or the interaction of the coal with the other cell components. The results show that the carbon content, the carbonaceous structure and the reactivity of the coals are key characteristics for optimal electrochemical behaviour. The plasticity of bituminous coals, an important parameter overlooked in previous works, can help to extend the area for electrochemical reactions beyond the current collector/anode interface. The reaction mechanism proposed shows that additional gas phase electrochemical reactions are an important contribution during the early stages of the electrochemical testing and that the direct electrochemical oxidation of solid carbon is the dominant reaction at longer times.

Received 00th January 20xx,
Accepted 00th January 20xx

DOI: 10.1039/x0xx00000x

www.rsc.org/

Broader Context

The intrinsic complexity of systems such as HDCFCs is further increased when coals are used as fuels due to their heterogeneous nature. There is a need for a deeper understanding of this type of fuel cell in order to achieve their commercial implementation. This work sheds new light on the reaction mechanism of the HDCFC operated with mineral coals by providing a systematic analysis of a series of comparable materials which have been thoroughly characterised and tested. Hard coals are promising candidates as they represent about 50% of the proven recoverable world coal reserves, and they have higher carbon content and higher conductivity than less mature coals. To enhance their electrochemical performance, other desirable properties can be obtained by using appropriate pre-treatments. The study shows that thermal pre-treatments of hard coals are not recommended for use in HDCFCs. However, oxidation treatments can help to improve the reactivity of anthracite coals (low H/C ratio). Concerning bituminous coals, the modification of their fluidity with the pre-treatment should be also taken into account, as this can reduce the contact area with other cell components and, thus, its performance. The results from this study pave the way for the selection of specific coals as fuels and possible pre-treatments for an enhanced performance in HDCFCs.

1. Introduction

Coal is a reliable and competitive fuel for which global demand continues to increase despite a recent tendency in many countries to reduce reliance on it as an energy source, partly due to the new global strict climate targets. Thus, even if other hydrocarbons and renewable sources gain importance, coal remains a strategic

resource for many energy uses as its reserves are available worldwide. In fact, it has been estimated that there are over 847 billion tonnes of proven coal reserves worldwide and that recoverable reserves are present in around 70 countries.¹ From the proven recoverable coal reserves worldwide, around 53% correspond to hard coal (anthracite, bituminous), 30% to sub-bituminous and only 17% to lignite.¹ Moreover, 90% of the coal produced worldwide is hard coal and only 10% is brown coal/lignite.¹ However, the energy applications of the coals must face the challenge of developing more efficient and environmental-friendly technologies, such as Direct Carbon Fuel Cells (DCFCs).

DCFCs operate on the same electrochemical principles as conventional fuel cells but using solid carbon as fuel, which is directly converted into electrical energy. There are different types

^a School of Chemistry, University of St. Andrews, Fife KY16 9ST, United Kingdom.

^b Instituto Nacional del Carbón (CSIC). C/ Francisco Pintado Fe N° 26, 33080, Oviedo, Spain.

† Corresponding author
Phone: +44 1334463817
Fax: +44 1334463808
e-mail: jtsi@st-andrews.ac.uk
DOI: 10.1039/x0xx00000x

of DCFCs depending on the type of electrolyte used, such as molten carbonate (MCFC), molten hydroxide (MHFC), solid oxide (SOFC) and hybrid direct carbon fuel cells (HDCFCs).²⁻⁴ Even though the interest in DCFCs has risen in general, nowadays most of the publications focus on the MCFC⁵⁻¹⁰ and SOFC,^{11,12} and much less information is available about HDCFC¹³⁻¹⁵ or MHFC.^{16,17} The HDCFCs contain two different electrolytes: a molten carbonate, which is mixed with the carbon source in the anode chamber, and a solid oxide electrolyte that separates the anode and the cathode.¹⁸ Thus, the HDCFCs are a combination of SOFCs and MCFCs, and aim to mitigate some of the problems associated with each cell type and to combine their advantages. For this reason, the HDCFCs are a very interesting option for commercial applications.

Studies reported so far about DCFCs have put much emphasis on analysing the influence of the fuel properties on the cell performance. Due to the complexity of these systems that operate with solid fuels, especially in the case of HDCFCs where two electrolytes are present, carbons or homogeneous carbon materials with very well-known properties are normally used, such as activated carbons, carbon black or graphite. However, as some researchers have pointed out, real world fuels, such as coals, should be investigated in order to achieve the industrial application of the DCFCs.⁴ In this regard, studies evaluating different fuel possibilities, like biomass, refuse fuels or coals, are beginning to emerge. However, the information currently available is still little and not sufficient to understand the reaction mechanism of DCFCs, especially in the case of HDCFCs. Therefore, a more systematic analysis is required to gain a deeper understanding of how properties of a material as heterogeneous as coal impact on the HDCFCs behaviour. This will help to determine the most appropriate coals and their possible pre-treatments to improve their electrochemical reactivity and, thereby, to finally achieve a commercial implementation of this technology.

In this paper, a comparative study of the HDCFC performance has been carried out with two different types of coal, a bituminous and an anthracite coal, and their carbonised and oxidised pre-treated counter-parts. Based on an exhaustive and comprehensive characterisation of the physical and chemical properties of the raw and pre-treated coals, coupled with the analysis of their electrochemical performance in an electrolyte supported HDCFC, a deep insight into the influence of different parameters regarded as determining factors, such as coal type, chemical composition, structure and other physical properties, is provided. Thereby, in this work, guidelines are provided to identify the optimal coal properties for enhanced performance as fuel in HDCFCs. On the other hand, the heating procedure used in the cell to reach the operating temperature can cause drastic changes in the coal structure and properties, as well as in the interaction of the coal with the carbonates. This aspect has been rarely taken into account when evaluating the performance of coals in HDCFCs. Thus, a systematic analysis of these factors (coal properties and coal-carbonates interactions) during the cell preparation was also accomplished for the raw coals. Moreover, in this work special attention has been paid to the plastic stage, a specific phenomenon that takes place when bituminous coals are used as fuels and which has been overlooked to date as far as we know. During this process, structural changes in plastic coals occur due to the transformation of the decomposing matrix from a solid to a solid-liquid-gaseous mixture (fluid-like viscous mass), and finally to a re-solidified phase.

The pre-treatments and the thermal processing during the cell preparation can affect this process.

2. Experimental

Two types of coals of different rank from Spanish basins have been used, a bituminous coal with medium volatile content (denoted B-M) and an anthracite coal (denoted A-M). In order to reduce the number of parameters affecting the performance of the HDCFC, the coals were milled and sieved to obtain the same particle size distribution (in the nomenclature of the samples, M refers to samples milled to lower than 75 µm).

2.1. Coal pre-treatments and coal preparation for cell testing

Carbonisation and oxidation pre-treatments were applied to the raw coals to modify their physico-chemical properties and analyse how these changes would affect their behaviour on the HDCFC system.

During the carbonisation pre-treatment, the coals were subjected to a heating process up to 750 °C in a nitrogen atmosphere (20 ml/min) at a ramp rate of 5 °C/min and kept at this temperature for 1 h. The carbonised samples were named C-B-M and C-A-M for the bituminous and the anthracite coals, respectively. The second pre-treatment consisted of an oxidation process and it was chosen to evaluate the influence of the oxygen functional groups. Different oxidation methods, such as air oxidation or oxidation with ammonium persulfate under reflux, were investigated. The highest oxidation was achieved with air, which is also the simplest method (13.7 wt. % of O with air oxidation vs. 7 wt. % of O with ammonium persulfate oxidation for B-M for example), so this method was selected for the study. Thus, five grams of the coal were treated in air (50 ml/min) at a ramp rate of 10 °C/min to 350°C and held at this temperature during 2 h. The oxidised samples were named O-B-M and O-A-M.

Eutectic mixtures of carbonates with different melting points are frequently used as a second electrolyte in HDCFCs, with lithium and potassium carbonates being the most common. A mixture of 62 mol% lithium carbonate (Aldrich Chemical Co. WI, USA) and 38 mol% potassium carbonate (Fisher, UK) was pre-mixed by ball milling in acetone for 24 h. Previous works¹⁹ show that 25 wt. % of carbonate is the optimal proportion of (Li-K)₂CO₃ in the coal-carbonates mixture for operating the HDCFC. Therefore, the raw, carbonised and oxidised samples were mixed with the carbonates mixture at a weight ratio 4:1. The mixture was dried in an oven at 80 °C overnight. A 2 g mixture of coal-carbonates was used in each experiment.

The Table 1 presented below lists the abbreviations and the details of each sample used in this work.

Energy and Environmental Science

PAPER

Table 1. Abbreviations and description of the samples used in this work.

Code	Sample description
A-M	Anthracite coal (raw)
B-M	Bituminous coal (raw)
C-A-M	Carbonised anthracite coal
C-B-M	Carbonised bituminous coal
O-A-M	Oxidised anthracite coal
O-B-M	Oxidised bituminous coal
(Li/K) ₂ CO ₃	Lithium (62mol%) and potassium (38mol%) carbonate mixture
(A-M+CO ₃ ²⁻)	Mixture of the raw anthracite coal and the carbonates mixture
(B-M+CO ₃ ²⁻)	Mixture of the raw bituminous coal and the carbonates mixture
(Li/K) ₂ CO ₃ -C*	Lithium and potassium carbonate mixture after the heating step to the working temperature of the fuel cell
A-M-C*	Raw anthracite coal after the heating step to the working temperature of the fuel cell
B-M-C*	Raw bituminous coal after the heating step to the working temperature of the fuel cell
(A-M+CO ₃ ²⁻)-C*	Mixture of the raw anthracite coal and the carbonates mixture after the heating step to the working temperature of the fuel cell
(B-M+CO ₃ ²⁻)-C*	Mixture of the raw bituminous coal and the carbonates mixture after the heating step to the working temperature of the fuel cell
M	Refers to coals milled to particle sizes lower than 75 μm
*	Process simulated ex-situ the fuel cell, in a tube furnace

2.2. Fuel characterisation

The particle size distribution was determined by Coulter analysis (LS13320, Beckman with the ALM water module). The chemical composition of the raw and pre-treated coals was determined by ultimate analysis (C, H, N, S, O wt. % content) and proximate analysis (volatiles, ash and moisture wt. % content). The analysis of C, H and N was performed in a LECO CHN 2000 according to the standard ASTM D-5373. The analysis of sulphur was carried out in a LECO S632 according to the standard ASTM D-4239, whereas the analysis of oxygen was performed in a LECO TRUSPEC Micro-O. Proximate analysis (volatile matter, ash and moisture content) was carried out in a LECO TGA-601 apparatus. The moisture and ash contents were determined following the standard ASTM 7582, and the volatile matter content following the ISO562. The reactivity of the samples was evaluated by means of thermogravimetric analysis (TGA) in a Q5000 IR (TA Instruments) thermobalance. The weight loss profile was determined by increasing the temperature up to 1000 °C at a rate of 10 °C/min under a gasification atmosphere (*i.e.* 20 ml/min CO₂). The nature of the oxygen functional groups was characterised by Fourier transform infrared spectroscopy (FTIR) in a Nicolet FTIR 8700 with the diffuse reflectance module Smart Collector. The data were recorded between 4000-650 cm⁻¹, using 100 scans and a resolution of 4 cm⁻¹. Temperature-Programmed Desorption (TPD) experiments were carried out on a Micromeritics AutoChem II analyser coupled to a mass spectrometer (OmniStar Pfeiffer) in order to monitor the amount of CO, CO₂ and H₂O desorbed from the samples when they are heated up to 1000 °C under an argon (50 cm³/min) atmosphere at 10 °C/min. Room temperature powder X-Ray Diffraction (XRD) analyses were performed using a PANalytical Empyrean diffractometer with Cu-Kα radiation in reflection mode during 2 hours in the region 2θ~10°-

90°. The obtained XRD patterns were analysed with STOE WinXPOW and HighScore Plus databases.

2.3. HDCFC experimental setup and cell fabrication

The two-electrode cell system used for the evaluation of the electrochemical performance of the coals is shown in Figure 1, and has been used in a previous work.²⁰ The structure of the electrolyte supported cell consists of a NiO(Aldrich, 325 mesh)-YSZ(Tosoh, TZ-84) anode, a YSZ electrolyte and a LSM((La_{0.8}Sr_{0.2})_{0.95}MnO_{3-δ}(Piche)))-YSZ cathode. The YSZ electrolyte pellets (thickness of 1 mm and diameter of 20 mm) were prepared by the dry-pressing method and sintered at 1500 °C for 10 h. The NiO-YSZ composite anode ink (NiO/YSZ=60:40 wt. %) was then screen printed on one of the sides of each YSZ electrolyte pellet, followed by sintering at 1350 °C for 2 h. Afterwards, the LSM-YSZ composite cathode ink (LSM/YSZ=50:50 wt. %) was screen printed on the other side, followed by sintering at 1100 °C for 2 h. Silver paste was painted on both electrodes following a grid pattern to act as a current collector, *i.e.* to guarantee a sufficient contact area for good electron collection and transfer. The cells were then treated at 800 °C for 1 h. A diagram of the cell design can be also seen in Fig. 1. The total active area of the cell was 1.13 cm². Once the cell was ready, it was sealed on an alumina tube using a ceramic sealant (Aremco 552) with the anode side up. The carbon-carbonates mixture was deposited on top of the anode side of the cell (Fig. 1). A gas flow rate of 15 ml/min of nitrogen was used in the anode side, whereas 200 ml/min of air was used in the cathode side. Nitrogen was selected as the purging gas over CO₂ to avoid the promotion of Boudouard reaction as this would lead to a reduction of the electrochemical efficiency since more carbon would be consumed through chemical reactions than

through electrochemical reactions. The working temperature of the cell was 750 °C.

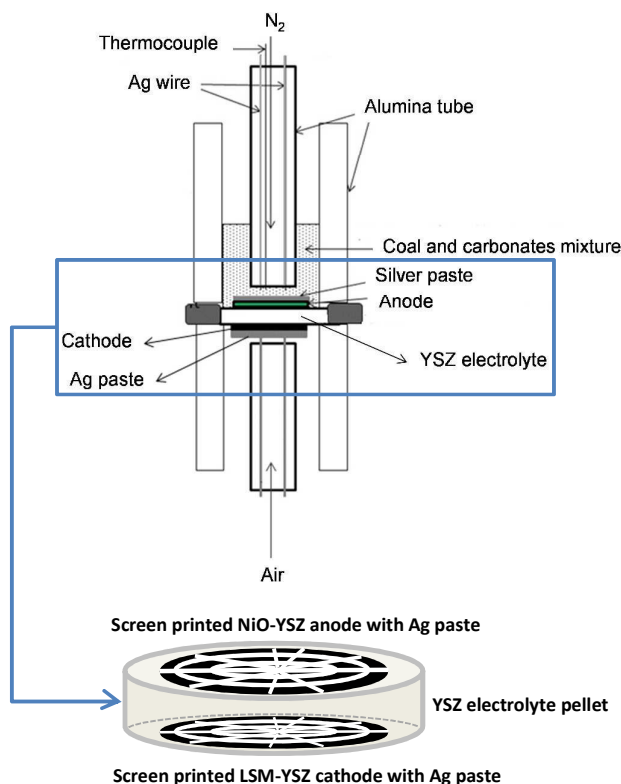


Figure 1. Diagram of the HDCFC setup and the cell design.

2.4. Fuel cell testing protocol

The fuel (*i.e.* coal) mixed with the carbonates is placed inside the anode chamber at room temperature. The cell is then heated with a ramp rate of 5 °C/min to 750 °C while a flow of inert gas (20 ml/min of N₂) passes through the anode chamber. During this heating procedure three steps are followed: (i) the cell is kept at 100 °C for *ca.* 30 minutes to dry the samples; (ii) it is then heated up to 250 °C, and maintained at this temperature *ca.* 30 minutes; (iii) and finally it is heated up to 750 °C and maintained for approximately another 30 minutes until the operating conditions are stabilised. Therefore, the overall heating process lasts nearly 4 hours. Afterwards, the electrochemical testing can be started. The electrochemical characterisation was performed with a Solartron 1280B and consisted of polarization (current-voltage) curves and stability tests (current output under 0.7 V potential).

3. Results and discussion

3.1. Influence of the heating step during the cell preparation

Few authors have considered the transformations, caused by the temperature increase and the interactions with the carbonates, that the coal can undergo during the unavoidable heating step of the cell prior to electrochemical testing.⁶ In fact, the fuel that undergoes the electrochemical testing is already likely to be a semi-coke or char, depending on whether it has undergone a plastic stage (bituminous) or not (lignites and anthracites) during the

heating process. To evaluate this process, and understand the consequences it has on the electrochemical mechanism, we have performed an ex-situ replication of this heating step in a tube furnace with the raw coals, the carbonates mixture and the raw coals mixed with the carbonates. The coal samples obtained after this process are denoted A-M-C and B-M-C, the carbonates mixture (Li/K)₂CO₃-C and the coal and carbonates mixtures (A-M+CO₃²⁻)-C and (B-M+CO₃²⁻)-C (see Table 1).

By comparing the results from the characterisation of the different materials before and after the heating process, which is an unavoidable step of the cell testing protocol with HDCFCs, it is possible to analyse the transformations of both the raw coals and the carbonates and the interactions between them. This characterisation provides information about the properties of the materials that would then undergo the electrochemical reactions in the actual fuel cell.

Table 2 summarizes the results from the proximate analysis, *i.e.* fixed carbon (FC), volatile matter (VM) and ash contents expressed in dry basis (db), and the ultimate analysis, *i.e.* the content of C, H, N, S and O expressed in dry ash free basis (daf), for the raw coals and the coal and coal/carbonates mixtures prepared in a tube furnace according to the heating procedure of the fuel cell described in the section 2.4 of this manuscript.

The proximate and ultimate analysis of the anthracite coal after heating to 750 °C (A-M-C) are similar to the ones of the raw coal (A-M), indicating that the heating step during the cell preparation does not notably modify the anthracite coal. The most relevant changes are the decrease of the volatile matter and oxygen contents (Table 2). For B-M the heating process leads to a large decrease of its volatile content (*i.e.* from 18.5 wt. % to 1.6 wt. %). As a consequence of the volatile matter evolution, the oxygen and hydrogen contents decrease to around 1 wt. % in B-M-C and at the same time the carbon content increases. The ash content is not modified during the thermal treatment, but with the release of volatiles the percentage of ash increases (see Table 2). When the carbonates are present during the heating procedure to 750 °C, the oxygen content of the remaining solids, (A-M+CO₃²⁻)-C and (B-M+CO₃²⁻)-C, is considerably higher than that of A-M-C and B-M-C (nearly 15 wt. % in both cases, Table 2). Also, in comparison with A-M-C and B-M-C, the carbon content of (A-M+CO₃²⁻)-C and (B-M+CO₃²⁻)-C is lower and their volatile matter and ash content are significantly higher (Table 2). It is worth noting that although both raw coals, B-M and A-M, have different compositions, (A-M+CO₃²⁻)-C and (B-M+CO₃²⁻)-C show very similar proximate and ultimate analyses but their electrochemical behaviour is very different, as it will be discussed in the next sections.

Energy and Environmental Science

PAPER

Table 2. Proximate and ultimate analysis of the raw coals (A-M and B-M) and these coals and their mixtures with carbonates after the heating process to the working temperature (750 °C) of the fuel cell, which has been simulated ex-situ in a tube furnace, (A-M-C, B-M-C, (A-M+CO₃²⁻)-C and (B-M+CO₃²⁻)-C).

Sample	Proximate analyses (wt. %)				Ultimate analyses (wt. %, daf)				
	FC (db)	VM (db)	Ash (db)	Moisture	C	H	N	S	O
A-M	85.8	4.1	10.1	2.4	93.1	2.0	0.9	1.0	3.0
A-M-C	89.1	1.2	9.7	0.7	96.0	1.5	1.1	1.0	0.4
(A-M+CO ₃ ²⁻)-C	60.1	16.4	23.5	2.7	81.2	0.9	1.6	1.0	15.3
B-M	77.4	18.5	4.1	0.8	89.6	4.6	1.6	0.7	3.5
B-M-C	90.3	1.6	8.1	0.7	95.5	1.3	1.7	0.7	0.8
(B-M+CO ₃ ²⁻)-C	60.0	20.6	19.4	2.6	81.6	0.9	2.5	0.5	14.5

daf: dry ash free basis

db: dry basis

In addition to the ultimate and proximate analyses, XRD studies were performed to obtain more information about the coal transformations and coal-carbonates interactions, Figure 2.

For the carbonate mixture, lithium carbonate (Li₂CO₃) and potassium carbonates hydrates (K₂CO₃·1.5H₂O and K₄H₂(CO₃)·1.5H₂O) are identified in the initial mixture (Fig. 2(a)). After the thermal treatment of the carbonates mixture, lithium potassium carbonate (LiKCO₃) and Li₂CO₃ are identified (Fig. 2(b)). In the case of the anthracite coal A-M, peaks corresponding to quartz and aluminosilicates are identified (see Figure 2(a)), which is coherent with its ash composition (61 wt. % of SiO₂ and 22 wt. % of Al₂O₃). For the bituminous coal B-M, no peaks of mineral matter were observed as it has a low ash content (4.1 wt. %), so its spectrum is not shown in Fig. 2 (a). In the (A-M+CO₃²⁻) mixture, the mineral compounds of the raw coal (quartz, aluminosilicates) plus the compounds of the carbonate mixture (Li₂CO₃, K₂CO₃·1.5H₂O) have been identified (Fig. 2(a)). For the (B-M+CO₃²⁻) mixture, only the peaks of the carbonates were identified, as expected. After the ex-situ pyrolysis of (A-M+CO₃²⁻) and (B-M+CO₃²⁻) to simulate the heating step in the fuel cell, the spectra are particularly complex due to the numerous overlapping peaks, which has hindered the identification of some of them (Fig. 2(b)). Nevertheless, for (A-M+CO₃²⁻)-C, K₂CO₃·1.5H₂O and SiO₂ (quartz) seem to be present. Similar compounds were found for (B-M+CO₃²⁻)-C, *i.e.* K₂CO₃·1.5H₂O, SiO₂, but also Fe. The identification of mineral components that were not visible in B-M, such as SiO₂ and Fe, is possible owing to a dual factor: i) the increase of the mineral matter content due to the removal of the volatile matter during the thermal treatment of the coal and ii) the reducing character of the carbon.

It is worth noting that K₂CO₃ is clearly identified in the XRD patterns of the coal-carbonates mixtures after the heating step, but not Li₂CO₃. Many studies indicate that the decomposition of the carbonates takes place around their melting point, whereas others note thermal instability and varying degrees of dissociation at temperatures lower than their melting point.²¹ The melting point of K₂CO₃ is around 900 °C, while the one of Li₂CO₃ is approx. 723 °C and the one of the eutectic mixture is around 488-503 °C.^{21,22} Furthermore, it has been reported that the decomposition degree is higher for Li₂CO₃ than for K₂CO₃ at temperatures higher than 700 °C in a N₂ atmosphere.²³ At temperatures higher than 700 °C, the gasification of coal due to the presence of carbonates can also occur and it can proceed via different mechanisms depending on the type of alkali metal carbonate. The specific gasification reactions depending on the carbonate type are out of the scope of this paper but more information can be found in the review published by Deleebeek and Hansen.²⁴ In our study, the fact that Li₂CO₃ is identified in the XRD spectrum of the heat-treated carbonates mixture but not in the XRD spectrum of the heat-treated (coal-carbonates) mixtures (Fig. 2) and the results of the proximate and ultimate analyses (Table 2) seem to indicate that a partial decomposition of some carbonates, mainly of Li₂CO₃, can occur during the heating step for the cell preparation, due to the high temperature and also the possible secondary reactions with the coal.

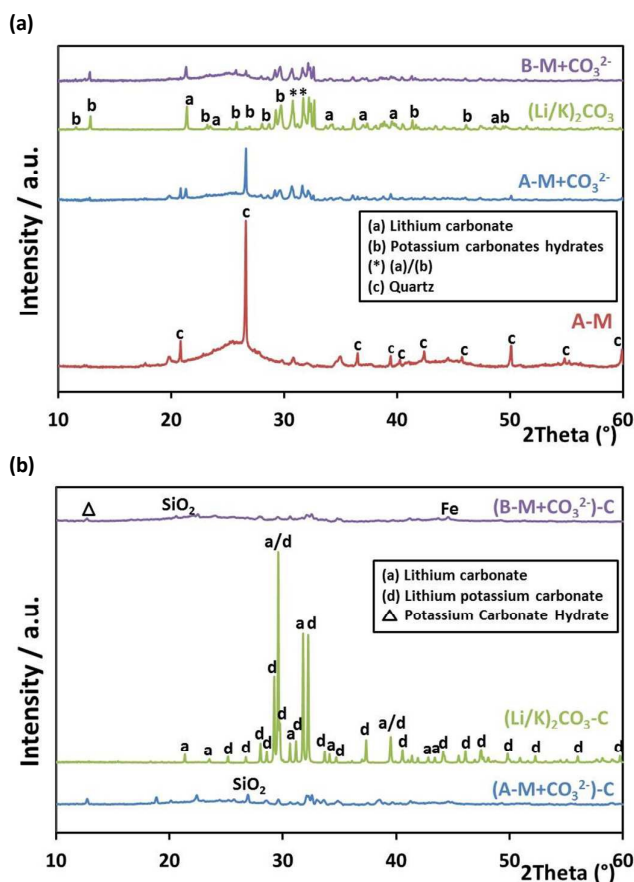


Figure 2. XRD of the (a) samples before the heating step, A-M, $(\text{Li/K})_2\text{CO}_3$, $(\text{A-M}+\text{CO}_3^{2-})$ and $(\text{B-M}+\text{CO}_3^{2-})$ and (b) samples after heating step, $(\text{Li/K})_2\text{CO}_3\text{-C}$, $(\text{A-M}+\text{CO}_3^{2-})\text{-C}$ and $(\text{B-M}+\text{CO}_3^{2-})\text{-C}$, which has been simulated ex-situ in a tube furnace.

Finally, Figure 3 shows the impact of the presence of the carbonates on the reactivity (towards Boudouard gasification) of the coals after the simulated heating step. As can be seen, the carbonates do not decompose in a CO_2 atmosphere, since the weight loss measured at low temperatures (below $200\text{ }^\circ\text{C}$) is due to the loss of moisture. This finding is in agreement with other studies which have reported no weight losses from carbonates in a CO_2 atmosphere.²³ Similarly, the reactivity of B-M-C and A-M-C is very low. However, the (coal+carbonates)-C samples present a very high reactivity at $T \geq 650\text{-}700\text{ }^\circ\text{C}$. In fact, the (coal+carbonates)-C samples react completely with CO_2 at around $900\text{ }^\circ\text{C}$, as revealed by the plateau observed above this temperature. These TGA results show that the presence of carbonates greatly catalyses the gasification reaction of the carbon source with CO_2 even after the coal-carbonates mixture have been subjected to a heating process. Therefore, if the partial pressure of CO_2 is sufficient during the electrochemical testing, the carbon gasification can occur more rapidly than the carbonate decomposition.²³

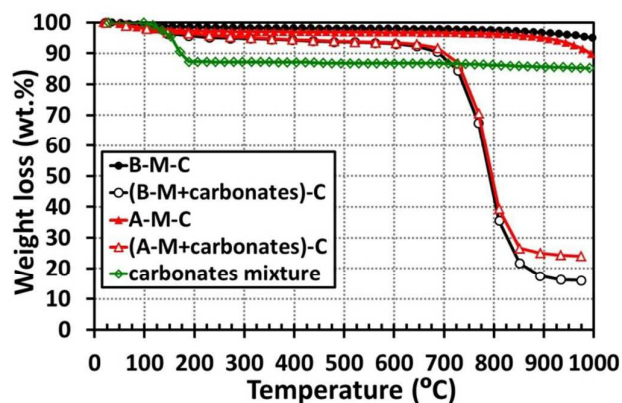


Figure 3. Reactivity in CO_2 atmosphere of the initial carbonates mixture, and of the raw coals and raw coals-carbonates mixture after the heating step simulated in the tube furnace (B-M-C, A-M-C, $(\text{B-M}+\text{CO}_3^{2-})\text{-C}$, $(\text{A-M}+\text{CO}_3^{2-})\text{-C}$).

3.2. Influence of coal carbonisation pre-treatment on the electrochemical performance in HDCFC

In this section the evolution of the coals characteristics upon the carbonisation pre-treatment and their impact on the cell performance is discussed.

The average weight loss of A-M during the carbonisation to obtain C-A-M is approximately 7.6% and that of B-M to produce C-B-M is around 17.2%. Table 3 shows a comparison of the C content and the atomic ratios H/C and O/C derived from the ultimate analysis (daf) for the raw and carbonised coals. The atomic ratios O/C and H/C decrease after the carbonisation pre-treatment for both coals, as the release of the volatile matter during this process mostly results in a reduction of the oxygen and hydrogen contents. The two atomic ratios are very similar for both carbonised samples, even though the initial H/C ratio of B-M is much higher than the one of A-M (Table 3). Finally, the carbon content of both coals increases slightly during the carbonisation as can be seen in Table 3.

Table 3. Carbon content (wt. %) and atomic ratios O/C and H/C of the pre-treated coals (carbonised and oxidised) in comparison to the raw coals.

Sample	C	O/C	H/C
A-M	93.1	0.024	0.256
C-A-M	95.0	0.010	0.176
O-A-M	84.4	0.104	0.268
B-M	89.6	0.029	0.612
C-B-M	95.2	0.011	0.150
O-B-M	81.0	0.127	0.441

Figure 4 compares the reactivity of the carbonised coals with that of the raw coals. This reactivity could provide an indication of the availability of active sites in the coal samples for chemical and electrochemical reactions. The weight losses that are observed

during these analyses can be ascribed to: i) the evolution of volatile matter as a consequence of the increase in temperature (mainly at temperatures below 700 °C) or ii) to the reaction with CO₂ (mainly at temperatures above 700 °C). The weight loss below 700 °C is much lower for A-M than for B-M, as the volatile matter content of A-M (4.1 wt. %) is much lower than the one of B-M (18.5 wt. %) (Table 3). For the carbonised coals, there are almost no weight losses up to 900 °C, as most of the volatile matter has been released during the pre-treatment. At the working temperature of the fuel cell, *i.e.* 750 °C, the reactivity of the coals after the carbonisation treatment is lower than the one of the raw coals (see insert graphic in Figure 4). This difference is particularly significant for the bituminous coal, which is consistent with its lower rank.

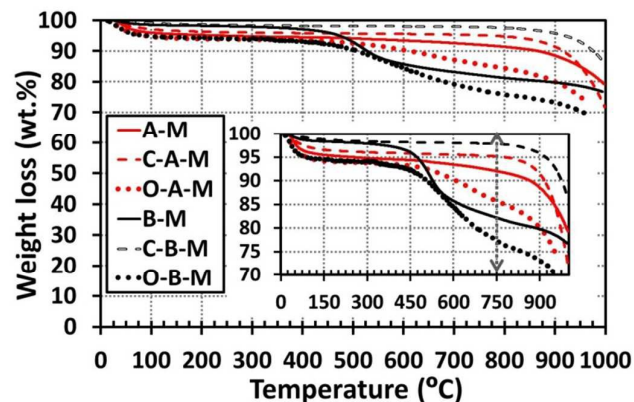


Figure 4. Reactivity of the raw, carbonised and oxidised coals in CO₂ atmosphere (the double arrow line in the insert graphic indicates the working temperature of the fuel cell, 750 °C).

The electrochemical performance (P-I-V curves) for the raw and carbonised coals in the HDCFC at 750 °C is presented in Figure 5. In these cells the anode processes are the rate limiting step. The cell operated with the bituminous coal B-M shows a polarization resistance (R_p) of 1.25 $\Omega \cdot \text{cm}^2$, while the polarization resistance of the cathode is about 0.36 $\Omega \cdot \text{cm}^2$.²⁰ Therefore, the polarization resistance of the anode accounts for about 70% of the total polarization resistance. For the rest of the coals, which show worse behaviour in the HDCFC and therefore higher total polarization resistance, the anode processes are the limiting processes as well.

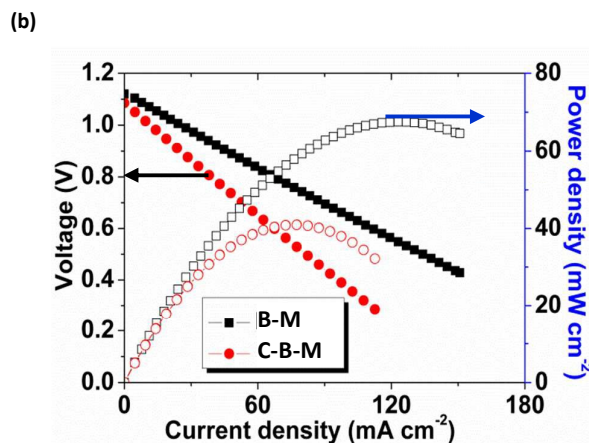
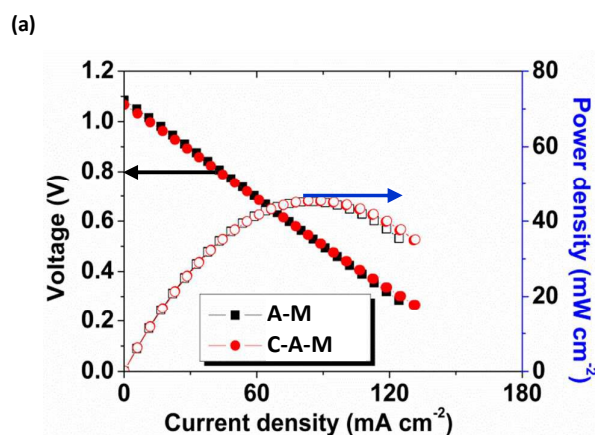


Figure 5. P-I-V curves at 750 °C of the (a) raw and carbonised anthracite coal (A-M and C-A-M) and (b) raw and carbonised bituminous coal (B-M and C-B-M).

When comparing the performance of the two raw coals, it can be observed that B-M exhibits much higher power density than A-M (67.5 $\text{mW} \cdot \text{cm}^{-2}$ vs. 45.2 $\text{mW} \cdot \text{cm}^{-2}$), even though the carbon content of B-M is lower than A-M (89.6 wt. % vs. 93.1 wt. %). Furthermore, for the raw coals, higher reactivity in CO₂ can be correlated with higher maximum power density at the working temperature (750 °C) of the fuel cell (see Fig. 4 and 5).

The results previously presented show that the carbonisation treatment did not lead to a significant change of the chemical composition and structure of A-M as it is already a well-developed coal (high aromaticity and less crosslinking). The small structural change is in agreement with the small loss of weight (7.6 wt. %) and the small change of the reactivity of the coal after carbonisation. Therefore, the electrochemical behaviour of A-M and C-A-M is analogous. The maximum power density is $\sim 45 \text{ mW} \cdot \text{cm}^{-2}$ for both samples and the OCV is 1.09 V for A-M and 1.07 V for C-A-M. On the other hand, the thermal treatment has a bigger impact on the bituminous coal and, therefore, a clear difference in the electrochemical behaviour of B-M and C-B-M can be observed. Fig. 5 (b) shows that C-B-M clearly exhibits worse electrochemical performance than B-M. The maximum power density of B-M is 67.5 $\text{mW} \cdot \text{cm}^{-2}$ whereas the one of C-B-M is 40.9 $\text{mW} \cdot \text{cm}^{-2}$. The OCV of B-M is 1.12 V and the one of C-B-M is 1.09 V. A relevant change must be taken into account when comparing the electrochemical behaviour of B-M and its carbonised derivative C-B-M. C-B-M underwent the plastic stage during the carbonisation treatment and, therefore, will not undergo it again inside the fuel cell during the electrochemical testing. This will significantly alter the interaction with the carbonates and the contact with the electrolyte, the current collector, etc. In fact, C-B-M has a more similar electrochemical behaviour to C-A-M and A-M. This is consistent with the similar chemical composition (Table 3), similar reactivity in CO₂ of both samples after the carbonisation, despite the different TGA profiles of the raw coals, and with the fact that the interaction of C-B-M with the carbonates, anode, electrolyte, etc. will be analogous to that of C-A-M or A-M (the three samples would be in a solid state during the whole process). Similarly to the results found with the raw coals, a slightly higher reactivity in CO₂ can be correlated with a slightly higher maximum power density for the carbonised samples (Figs. 4 and 5).

Two other properties of the coals could explain the different electrochemical performance observed: the surface area and the mineral matter. The coals samples (raw and pre-treated) present low surface areas ($\leq 50 \text{ m}^2/\text{g}$). Therefore, we consider that the different reactivity of these samples is not so much related to the different porosity and, hence, to gas diffusion, but to the different chemical composition. Moreover, the difference between their surface areas is not significant enough to be considered as a determining parameter when comparing their electrochemical performance. In relation to the influence of the mineral matter, other researchers have carried out studies with mineral coals and their carbonised counterparts in DCFC.²⁵ Allen *et al.*²⁵ have concluded that the ash type considerably influences the electrochemical performance when carbonised samples of high ash content are used. However, in our case the mineral coals used do not have a high ash content ($<10 \text{ wt. \%}$). Moreover, the ash content does not vary significantly between the raw and carbonised samples (or the raw and oxidised samples).

So, even if the carbon content is an important factor, these results stress the high importance of the structure of the coal (edge sites and defects) and the contact of the coal with other cell components on its electrochemical performance in HDCFC.

3.3. Influence of coal oxidation pre-treatment on the electrochemical performance in HDCFC

The oxidation pre-treatment allows studying the influence of the oxygen functional groups of the coals on their performance in the HDCFCs.

The C content and atomic ratios O/C and H/C of the oxidised coals are presented in Table 3 together with the raw and carbonised samples for comparison purposes. A slight decrease ($\sim 9\%$) of the carbon content can be observed for both coals upon oxidation. As the oxidation pre-treatment leads to an important increase of the oxygen content for both coals (from 3 to 11.4 wt. % for the anthracite coal and from 3.5 to 13.7 wt. % for the bituminous coal), the atomic ratio O/C increases for both coals (Table 3). The H/C ratio also increases for the anthracite coal as the H content (2 wt. %, Table 3) is almost not modified upon oxidation for this coal and the C content only slightly decreases, as mentioned previously (Table 3). A considerable decrease of the H/C ratio can be observed for the bituminous coal (Table 3) as the hydrogen content remarkably decreases upon oxidation for this coal (from 4.6 wt. % to 3 wt. %).

The reactivity of the oxidised coals towards Boudouard reaction (CO_2 atmosphere) is presented in Figure 4 together with the raw and carbonised samples for comparison purposes. The TGA results show that the oxidised coals are more reactive than the raw coals at 750°C . The higher reactivity of the oxidised coals can be explained by their higher content of labile volatile compounds (the new oxygen functionalities created during the process) which can easily evolve with the increase of the temperature, leaving active sites ready to react. It is worth noting that, after this pre-treatment, both oxidised coals seem to present the same type of behaviour in terms of reactivity in CO_2 , although O-B-M is more reactive than O-A-M.

The oxidation pre-treatment also causes important modifications of the volatile matter of the two coals as well as on the plastic properties of the bituminous coal. The proximate analysis shows that the volatile matter content increased from 4.1 wt. % to 23.6

wt. % for the anthracite coal and from 18.5 wt. % to 24 wt. % for the bituminous coal. The introduction of new oxygen functionalities more labile than the CH groups present in the original coal structure, such as carbonyl and carboxyl groups, can lead to an increase in the VM content (see IR results below). However, when the oxidation is performed during short periods of time the devolatilisation (thermal process) can compete with the chemisorption of oxygen groups and, therefore, even a decrease of the VM content of the coal could be observed. This factor would explain the differences observed in the increase of the VM depending on the type of coal. Finally, the oxidation of the caking coals is known to impact their fluidity, which is greatly reduced and can even be completely eliminated with the increase of the oxygen content.²⁶ In order to analyse this phenomenon and to help understanding the possible role of the oxygen functionalities in the reaction mechanism in the fuel cell, which will be discussed in the next section 3.4, the oxidised and raw coals were studied by FTIR spectroscopy and thermal programmed desorption (TPD).

The FTIR results are presented in Figure 6. The spectrum of A-M presents similar bands to B-M but the intensities are much lower as it is a more evolved coal. For comparison purposes, the intensity of the signals for A-M has been magnified by a factor of ten ($\times 10$). One of the main differences between the two raw coals is the band at *ca.* $3600\text{--}3700 \text{ cm}^{-1}$, corresponding to mineral matter. This band is more intense in the case of the anthracite coal (A-M) due to its higher mineral matter content ($\sim 10 \text{ wt. \%}$ vs. $\sim 4 \text{ wt. \%}$). For the anthracite coal, a clear increase of the bands at wavenumbers around 1641 , 1550 and 1259 cm^{-1} is observed after the oxidation treatment (*i.e.* O-A-M sample), see Fig. 6 (a). Regarding the bituminous coal, the oxidation also leads to an increase of the bands around 3400 , 1687 and 1261 cm^{-1} . The band around $3400\text{--}3500 \text{ cm}^{-1}$ is related to the O-H stretching, the one at $1600\text{--}1700 \text{ cm}^{-1}$ to C=O stretching and the one at 1260 cm^{-1} to C-O stretching and O-H bending. These bands confirm that the oxidation treatment has promoted the formation of carboxylic acids, ethers (1260 cm^{-1}) and lactones ($1640\text{--}1680 \text{ cm}^{-1}$ and 1260 cm^{-1}) for both coals. O-A-M presents a band around 1550 cm^{-1} which is not observed for O-B-M and that might be due to the presence of quinones.

Finally, the FTIR studies show an important structural change for the bituminous coal after oxidation. For O-B-M the bands related to the aliphatic hydrocarbons (1400 cm^{-1} for C-H bending modes and 2850 , 2920 , 2951 cm^{-1} for C-H stretching modes) significantly decrease, as well as the aromatic C-H absorption bands (region $748\text{--}866 \text{ cm}^{-1}$ for C-H out of plane bending modes and band at 3062 cm^{-1} for stretching of aromatic hydrocarbons). Therefore, it seems that the increase of the carbonyl and carboxyl functionalities is produced at the expense of both aliphatic and aromatic hydrogen, which is consistent with the decrease of H percentage of B-M after oxidation. It has been reported that a decrease in aliphatic CH groups produces a loss of plastic properties of bituminous coals, as the aliphatic hydrogen is a key factor in the development of the plasticity of the coal. Moreover, the formation of ethers during oxidation, which causes an increase in crosslinking, also plays an important role in the loss of plasticity.²⁶ Both phenomena are observed upon oxidation of B-M, therefore indicating the decrease of the plasticity of the coal.

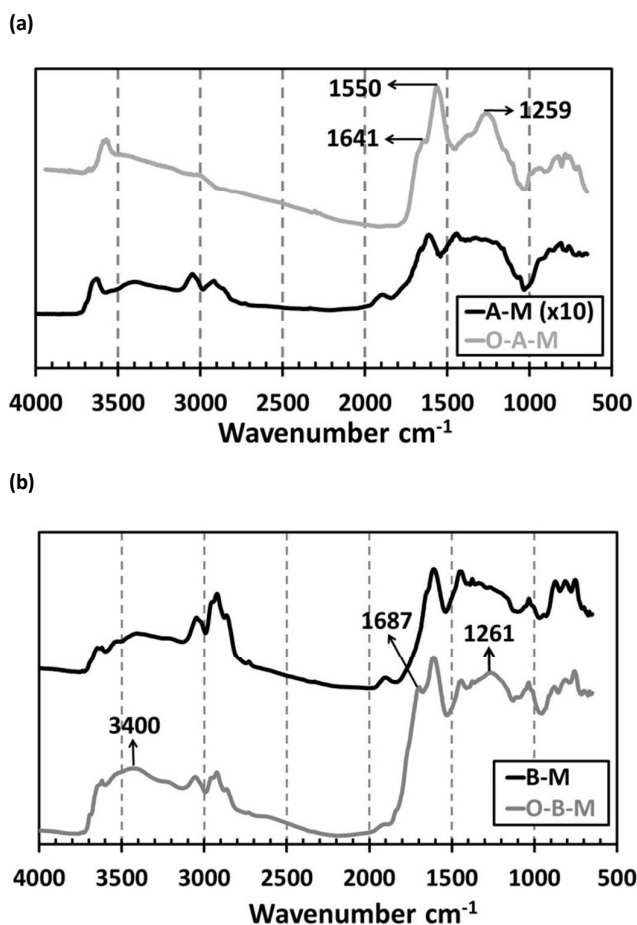


Figure 6. FTIR spectra of the (a) raw and oxidised anthracite coal (A-M and O-A-M) and (b) raw and oxidised bituminous coal (B-M and O-B-M). The intensity of the absorbance of A-M has been increased (x10) for comparison purposes.

Figure 7 shows the evolution of the (a) CO₂ and (b) CO gases from the oxidised bituminous (O-B-M) and oxidised anthracite (O-A-M) coals from the TPD analyses. The TPD analyses confirm that most of the oxygen groups created with this pre-treatment desorb as CO. However, a small amount of oxygen functionalities that decomposes as CO₂ are also present in the oxidised coals. In general terms, O-B-M has more oxygen functionalities than O-A-M, which is coherent with the results showed in Table 3. The CO₂ evolution from O-B-M presents a main peak around 482 °C with a shoulder at 542 °C. Moreover, the release of CO₂ for this sample starts before 400 °C as can be seen in Fig. 7 (a). Regarding the CO functionalities, two contributions are observed around 537 °C and 664 °C (Fig. 7 (b)). The release of CO₂ at temperatures lower than 400 °C indicates the presence of carboxylic acids. Moreover, the release of CO₂ and CO occurring at similar temperatures, 542 °C and 537 °C respectively, could be explained by the presence of anhydrides.²⁷⁻³⁰ It must be noted that the carboxylic groups can condensate into anhydride functional groups when they are very close to each other, which would explain the identification of carboxylic groups and anhydrides by TPD. However, the intensity of the CO peak at 537 °C is higher than the CO₂ peak at 542 °C, which can be due to the release of other oxygen functionalities at this temperature, such as carbonyl groups. Finally, the CO₂ peak at 482 °C may indicate the

presence of lactones and the CO peak at 664 °C of ethers.²⁷⁻³⁰ The CO₂ evolution from O-A-M also presents two contributions that appear at slightly higher temperatures than for O-B-M, *i.e.* 501 °C and 614 °C (Fig. 7 (a)), whereas the CO curve shows a peak around 634 °C with a shoulder at around 787 °C (Fig. 7 (b)). The CO₂ peak at 501 °C might be related to the presence of lactones. The presence of anhydrides in this sample is suggested by the overlapping of bands of very similar intensity of CO₂ at 614 °C and CO at 634 °C. Finally, the CO peak at 787 °C may be due to quinone groups, with some contributions from ethers or carbonyls.²⁶⁻²⁹ These TPD analyses are in agreement with the identifications done by FTIR (Fig. 6).

It is worth remarking that the TPD analyses demonstrate the presence of oxygen functionalities that desorb as CO at 750 °C (working temperature of the fuel cell), even though the CO₂ functional groups have been completely released (see Fig. 7 (a)). This is important as the CO(g) release during the cell testing can be involved in electrochemical reactions as will be discussed in the next section.

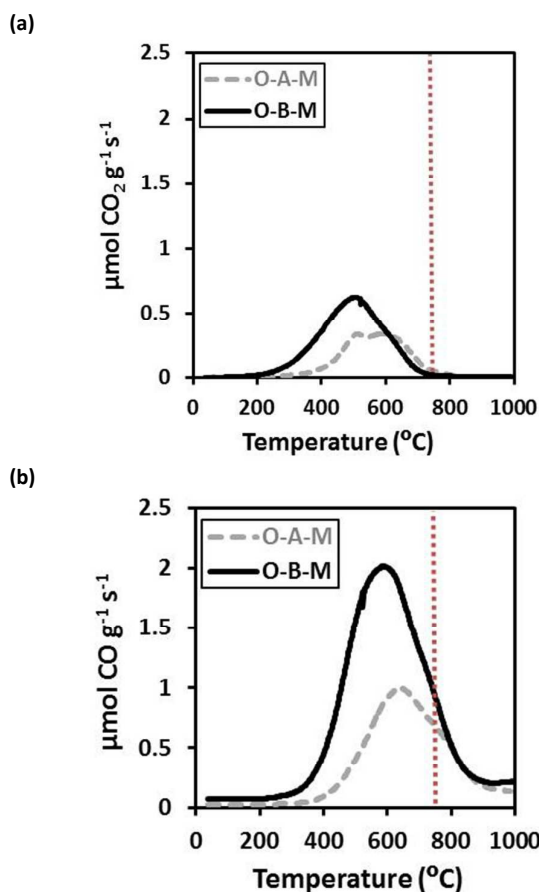


Figure 7. (a) CO₂ and (b) CO evolution determined by TPD from the oxidised coal samples, O-A-M and O-B-M. The vertical dotted lines indicate the working temperature of the HDCFC, 750 °C.

Finally, the electrochemical behaviour of the oxidised coals was evaluated via stability tests in the HDCFC under a potential of 0.7 V for 12 h at 750 °C and compared with that of the raw and carbonised coals. The results from these tests are given in Figure 8.

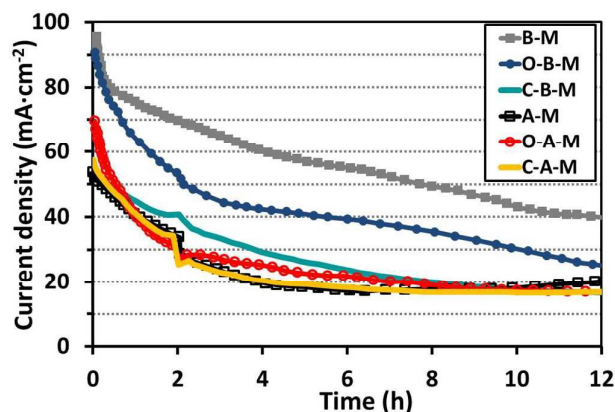


Figure 8. Stability tests of the oxidised, carbonised and raw anthracite and bituminous coals performed in the HDCFC under a potential of 0.7 V and 750 °C.

As can be seen in Fig. 8, two samples stand out among all the coals tested, B-M and O-B-M. The raw and oxidised bituminous coals have a very similar initial current density, but show a noticeable difference in the current output over time. In the case of the anthracite samples, O-A-M exhibits a higher initial current density than A-M, but over time their current densities become very similar. The current density of both oxidised coals decreases quicker than that of the raw coals during the first hours of operation. For O-A-M, the current density drops from ~ 70 to ~ 27 $\text{mA}\cdot\text{cm}^{-2}$ during the first 2 h, then continues decreasing at a slower rate down to ~ 22 $\text{mA}\cdot\text{cm}^{-2}$ after 5 h and finally reaches a stabilised value of around 17 $\text{mA}\cdot\text{cm}^{-2}$ after 8 h. For O-B-M, the current density drops from ~ 91 to ~ 52 $\text{mA}\cdot\text{cm}^{-2}$ in the first 2 h, it further decreases to ~ 41 $\text{mA}\cdot\text{cm}^{-2}$ after 5 h and it stabilises around ~ 24 $\text{mA}\cdot\text{cm}^{-2}$ at the end of the test. Concerning the behaviour of the carbonised samples during the stability tests, it can be seen that C-A-M shows a very similar behaviour to A-M, which is in agreement with their similar physico-chemical properties, whereas C-B-M is clearly behaving worse than B-M and O-B-M. Initially, C-B-M shows higher current output than C-A-M but, at longer testing times, their behaviours are similar. These results demonstrate that the pre-treatments can both impact the initial performance and the stability of a HDCFC.

Furthermore, a potential correlation between the properties of the coals and their electrochemical behaviour was investigated. A linear correlation was found between the initial and final current densities from the stability tests and the atomic H/C ratios for all the coal samples evaluated (see Figure 9), which reinforces the idea that the carbonaceous structure of the coals is another very relevant parameter when analysing the electrochemical behaviour of the mineral coals.

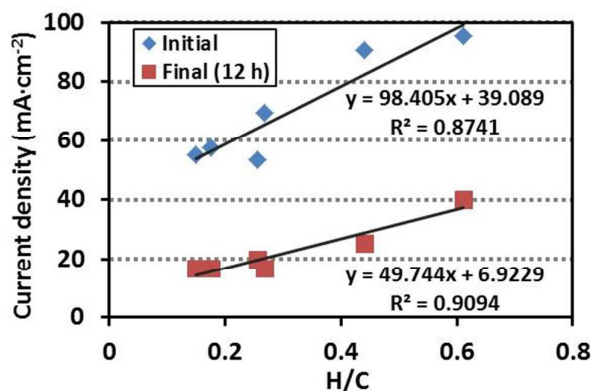


Figure 9. Correlations of the initial and final (12 h) current densities during the stability tests (0.7 V, 750 °C) with the atomic ratio H/C considering the raw and pre-treated coals as introduced into the cell.

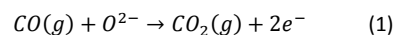
3.4. Reaction schemes as function of coal type

In this section, the possible reactions taking place in the fuel cell are assessed based on the properties of the different coal samples and the electrochemical results previously discussed.

The main reaction sought in HDCFCs is the direct electrochemical oxidation of C to CO_2 . The expected OCV value corresponding to this reaction is 1.02 V. Many authors have suggested that higher OCVs imply the presence of alternative reaction mechanisms through different mediators. The CO mediator has been suggested in HDCFCs that contain Ni in the anode. Another mediator system could be due to the decomposition of the carbonates. In fact, the decomposition of the carbonates has been reported to impact the OCV significantly, resulting in an increase up to 1.4 V at 900 °C.³¹ However, some authors consider that the incomplete oxidation of solid carbon (considered as part of the CO mediator system) or the Boudouard reaction will represent competing processes and, therefore, will decrease the likelihood of complete carbon oxidation and will not contribute to the increase of the OCV.²⁴

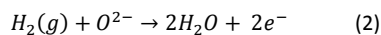
In our case, the OCVs measured are also higher than the theoretical value expected for the direct electrochemical oxidation of solid carbon to CO_2 , e.g. 1.12 V for the raw bituminous coal (B-M) instead of the 1.02 V expected. Therefore, this is an indication that reactions other than the direct electrochemical oxidation of C to CO_2 are taking place in the HDCFC.

The first mediator system that we have considered in our system is the oxygen functionalities. Both oxidised coals (O-A-M and O-B-M) have certain oxygen functionalities, which will be released mainly as $\text{CO}(\text{g})$, at the working temperature of the fuel cell, as shown by IR and TPD studies (Figs. 6 and 7). These oxygen functionalities could easily diffuse to the three phase boundary (TPB) and contribute to the CO mediator system via the electrochemical reaction (1). However, less oxygen functionalities are likely to be released from the raw and carbonised coal samples at the working temperature of the fuel cell, 750 °C.

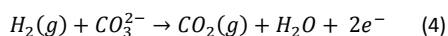
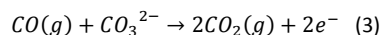


The second mediator system could be $\text{H}_2(\text{g})$. In section 3.1 it has been shown that an important part of the H_2 is evolved from the

(raw) coals during the heating step, *i.e.* before the electrochemical reactions are started. The remaining H₂ (Tables 2 and 3) can also be involved in electrochemical reactions such as the one shown in reaction (2), even if it is to a small extent.⁸ This contribution could be more significant for oxidised and raw coals than for the carbonised samples as H₂ is lost upon the carbonisation pre-treatment to a greater extent (Table 3).

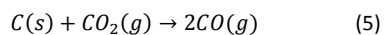


The electrochemical oxidation of CO(g) and/or H₂(g) released from the coals can also be promoted by the second electrolyte present in the HDCFC, *i.e.* the carbonates, according to reactions (3) and (4):



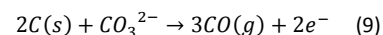
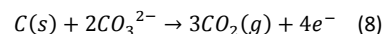
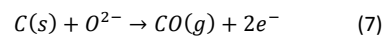
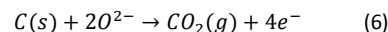
This additional oxidation of CO(g) and H₂(g) related to the intrinsic oxygen and hydrogen functionalities of the coal by oxygen ions and/or carbonates pathways could contribute to the increase of the theoretical OCV and provide higher current density outputs at the initial stages of the stability tests.

On the other hand, the competing chemical Boudouard reaction (5) can be significant in our system at 750 °C. The oxidised coals are likely to undergo Boudouard reaction to a greater extent than the raw and carbonised coals. According to the TGA studies performed, the oxidised bituminous coal (O-B-M) is the most reactive sample among all the coals evaluated (Fig. 4). The carbonised samples show very low reactivity towards Boudouard reaction (Fig. 4), due to the loss of most of the crosslinks, structural defects, VM, etc. during the carbonisation pre-treatment, which could be the active centres for this reaction. Therefore, by increasing order of importance, the samples with the highest loss of carbon due to Boudouard reaction would be the oxidised, the raw and finally the carbonised coals. Nevertheless, the presence of carbonates is one additional factor that has to be considered when analysing this reaction. The carbonates can clearly promote the gasification of all the coal samples even if their initial reactivity is low, as shown in Fig. 3. As N₂ is continuously supplied in the anode chamber we can suppose that the atmosphere will not be purely CO₂; however, this reaction can proceed quickly in the areas where the concentration of CO₂ is high, releasing more CO(g) that can undergo reactions (1) and/or (3).



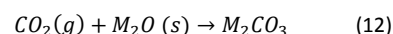
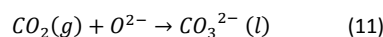
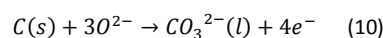
This could be the reason why the current density produced by the oxidised coals decreases much quicker than that of the raw or carbonised coals during the stability tests. The lack of active sites in the three phase boundary for the electrochemical reactions (1) and (3) to proceed could greatly compromise the cell performance, as the coal will be quickly consumed through Boudouard reaction but without producing any current. This could cause the current density to drop rapidly. Zhang *et al.*³² have also pointed out a degradation mechanism of a SOFC based on these two reactions but considering that it is the lack of CO(g) production from reaction (5) that will break the cycle balance. However, the results from the TG in CO₂ show the high reactivity of oxidised coals and, therefore, we think that reaction (5) could proceed quite quickly and will not be the limiting step.

At longer testing times, the electrochemical reactions of the solid carbon (reactions (6) to (9)) in the three phase boundary could in fact be the reactions that will maintain a stable current output during the stability tests:



The CO(g) from reactions (7) and (9) could be further involved in gas phase electrochemical reactions.

Finally, reactions for the re-generation of the carbonates such as (10) to (12), giving a CO₂ shuttle, should be considered:



The raw (B-M) and oxidised bituminous (O-B-M) coals produced the higher current density outputs during the stability tests. These samples share a common characteristic, *i.e.* certain fluidity, contrary to A-M, C-A-M and C-B-M. The raw bituminous coal (B-M) fully undergoes the plastic stage in the anode chamber. As the eutectic carbonate mixture melts at around 488-503 °C,^{21,22} B-M and the carbonates could both be in fluid state at some point. Once the working temperature for the electrochemical testing (750 °C) is reached, the coal is likely to be already re-solidified, as the re-solidification usually takes place from 500-550 °C. The transition of the coal through a liquid phase in the anode chamber might improve its distribution at the interface electrolyte(YSZ)-electrode(Ni) and also improve the mixture with the carbonates, favouring a more homogeneous dispersion of the carbonates in the coal matrix (coal:carbonates ratio is 4:1). The final result would be an increase of the active area of the three phase boundary for the electrochemical reactions (gas and solid phases). This could explain the higher current densities and slower degradation with time when comparing B-M with the rest of the coal samples. Moreover, B-M shows a remarkable maximum power density compared to other direct coal fuel cells operated with mineral coals even though a thick electrolyte is used for the electrochemical testing.^{4-8,12,17,33} In section 3.2 we have shown that the plasticity of the bituminous coal is clearly reduced after the oxidation pre-treatment. However, O-B-M still presents a slight fluidity which could explain its lower degradation during the stability tests compared to the rest of the coal samples (Fig. 8), and particularly compared to the oxidised anthracite, O-A-M, even though the reactivity of O-B-M is considerably higher than the one of O-A-M (Fig. 4).

Some authors have pointed out that in a DCFC the carbonates could probably work as an ion conductor and the carbon fuel itself as a current collector, in addition to the mesh. Consequently, the number of fuel-anode contacts and the carbon conductivity can have an effect on the behaviour of the cell.^{9,12,31} On the other hand, other authors have proposed that the electrochemical reaction zone for the direct carbon oxidation and carbonate-mediated oxidation modes is not spread into the entire anode (it is just

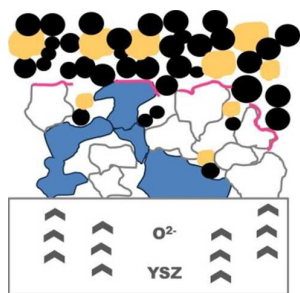
PAPER

Energy & Environmental Science

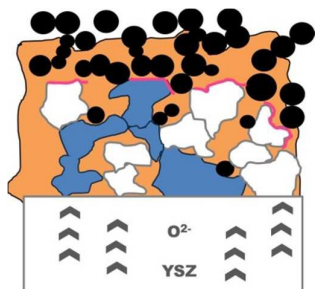
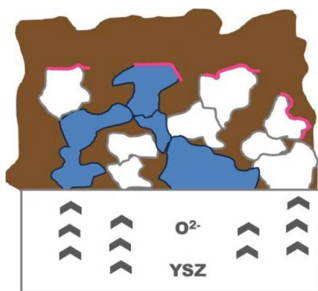
restricted to the two dimensional area on the anode surface) and the reaction zone for the CO oxidation mode is directly related to the anode surface area.²² It is clear that the electrochemical reaction will take place in the three (or perhaps four) phase boundary, but it is difficult to evaluate whether the contribution from the bulk of the sample, which is helped by the possible ion conductivity and electron conductivity of the carbonates and the coal, is relevant. However, in both schemes, it seems clear that the fluidity of the coal would help to increase the active reaction zone (points of contact between the fuel, electrode, solid electrolyte and molten carbonates) and enhance the electrochemical reactions.

Figure 10 shows how the system in the anode chamber may evolve with the temperature depending on the type of coal and, therefore, how the active reaction zone for electrochemical reactions may vary. From (a) to (b) and (c) we can see how the coverage is improving and, therefore, how the active zone may be extended.

(a) HDCFC at room temperature



(b) HDCFC at working temperature (750 °C) with raw anthracite (or lignite) and carbonised coals

(c) HDCFC at intermediate temperatures with the raw bituminous coal. Melting point of CO₃²⁻ and plastic stage bituminous coal

(d) HDCFC at working temperature (750 °C) once the raw bituminous coal is re-solidified

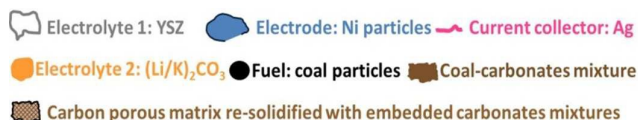
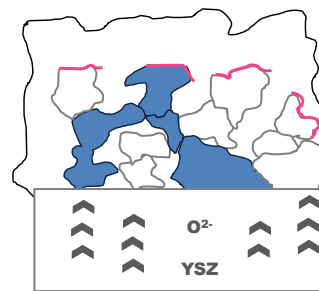


Figure 10. Schematic illustration of anode chamber depicting the possible active reaction zone of the HDCFC operated with coals in function of the temperature and type of coal: (a) initial situation in HDCFC at room temperature for all type of coals, (b) situation of HDCFC with raw anthracite (or lignite) and carbonised coal samples at working temperature (750 °C), (c) situation at intermediate temperature when the bituminous coal and the carbonates mixture reach the fluid point and (d) situation at 750 °C with the raw bituminous coal. The oxidised bituminous coal could be in an intermediate situation between raw and carbonised bituminous coals depending on how much its plasticity is reduced during the oxidation pre-treatment.

Conclusions

The results from this work show that the bituminous or oxidised anthracite coals are good options as fuels for HDCFC. The maximum power density of the HDCFC is higher when using raw bituminous compared to raw anthracite or raw coals instead of carbonised samples. Therefore, the higher the aromaticity of the coal – understood as an increase of the sp² carbon and represented in the coals by higher carbon content of higher structural order and lower H/C ratio – the lower the maximum power density of the HDCFC. Consequently, thermal treatments of high rank coals are not recommended. Oxidation pre-treatments can improve certain characteristics of the anthracite coals, such as oxygen content or reactivity. However, in the case of the bituminous coal, the creation of crosslinks and the reduction of aliphatic hydrogen during the oxidation pre-treatment reduce the fluidity of the coal and, therefore, reduce the active reaction area compared to the raw bituminous coal. A lower active reaction area and a higher reactivity of the oxidised bituminous coal seem to lead to a faster decline in the current output during stability testing. A reaction mechanism in the HDCFC was proposed depending on coal type and properties. In general, it was suggested that additional gas phase electrochemical reactions of CO(g) and H₂(g) by oxygen ions and/or carbonates mediators can be an important contribution at the early stages of the electrochemical testing. On the long term, the direct electrochemical oxidation of the solid coal seems to be the dominant reaction. The fluidity of the bituminous coals could be a beneficial property in batch operation mode of the HDCFCs as it can

promote an intimate contact at the electrochemical reaction sites. However, it could also be a handicap when operating in a continuous mode from the feeding point of view. Nevertheless, further research is needed and special attention will be paid to bituminous coals due to their unique plastic properties, which can have an important impact for this application.

Acknowledgements

The authors would like to acknowledge the financial support from the European project "Efficient Conversion of Coal to Electricity – Direct Coal Fuel Cells", which is funded by the Research Fund for Carbon & Steel (RFC-PR-10007), and the support from EPSRC Platform Grant EP/K015540/1, EPSRC and Royal Society Wolfson Merit Award WRMA 2012/R2. The authors would also like to thank the help of Dr. Jianjun Ma for the cell preparation.

References

1. www.worldcoal.org.
2. M. Muthuvel, X. Jin and G.G. Botte, *Encyclopedia of Electrochemical Power Sources*, 2009, 158.
3. T. M. Gur, *Chem. Rev.*, 2013, 113, 6179.
4. A. C. Rady, S. Giddey, S. P. S. Badwal, B. P. Ladewig and S. Bhattacharya, *Energ. Fuel*, 2012, 26, 1471.
5. X. Li, Z. Zhu, R. De Marco, J. Bradley and A. Dicks, *J. Phys. Chem. A*, 2010, 114, 3855.
6. S. Y. Ahn, S. Y. Eom, Y. H. Rhie, Y. M. Sung, C. E. Moon, G. M. Choi and D. J. Kim, *Appl. Energ.*, 2013, 105, 207.
7. S. Y. Ahn, S. Y. Eom, Y. H. Rhie, Y. M. Sung, C. E. Moon, G. M. Choi and D. J. Kim, *Energy*, 2013, 51, 447.
8. S. Y. Eom, S. Y. Ahn, Y.H. Rhie, K. Kang, Y. M. Sung, C. E. Moon, G. M. Choi and D. J. Kim, *Energy*, 2014, 74, 734.
9. X. Li, Z. Zhu, J. Chen, R. De Marco, A. Dicks, J. Bradley and G. Lu, *J. Power Sources*, 2009, 186, 1.
10. H. Watanabe, T. Furuyama and K. Okazaki, *J. Power Sources*, 2015, 273, 340.
11. J. Jewulski, M. Skrzyplikiewicz, M. Struzik and I. Lubarska-Radziejewska, *Int. J. Hydrogen Energy*, 2014, 39, 21778.
12. A. C. Rady, S. Giddey, A. Kulkarni, S. P. S. Badwal, S. Bhattacharya and B. P. Ladewig, *Appl. Energ.*, 2014, 120, 56.
13. W. Hao, X. He and Y. Mi, *Appl. Energ.*, 2014, 135, 174.
14. X. Xu, W. Zhou, F. Liang and Z. Zhu, *Appl. Energ.*, 2013, 108, 402.
15. X. Xu, W. Zhou, F. Liang and Z. Zhu, *Int. J. Hydrogen Energy*, 2013, 38, 5367.
16. L. Guo, J. M. Calo, C. Kearney and P. Grimshaw, *Appl. Energ.*, 2014, 129, 32.
17. A. Kacprzak, R. Kobyłcki, R. Włodarczyk and Z. Bis, *J. Power Sources*, 2014, 255, 179.
18. J. T. S. Irvine and co-workers, *Fuel Cell Bull.*, 2008, 10.
19. C. Jiang and J. T. S. Irvine, *J. Power Sources*, 2011, 196, 7318.
20. C. Jiang, J. Ma, A. D. Bonaccorso and J. T. S. Irvine, *Energy Environ. Sci.*, 2012, 5, 6973.
21. R.L. Lehman, J.S. Gentry, N.G. Glumac, *Thermochim. Acta*, 1998, 316, 1.
22. J.-Y. Lee, R.-H. Song, S.-B. Lee, T.-H. Lim, S.-J. Park, Y. G. Shul and J.-W. Lee, *Int. J. Hydrogen Energy*, 2014, 39, 11749.
23. J. Y. Hwang, J.H. Yu, K. Kang, *Curr. Appl. Phys.*, 2015, 15, 1580.
24. L. Deleebeeck, K.K. Hansen, *J. Solid State Electrochem.*, 2014, 18, 861.
25. J.A. Allen, M. Glen, S.W. Donne, *J. Power Sources*, 2015, 279, 384.
26. M.J. Iglesias, G. de la Puente, E. Fuente, J.J. Pis, *Vib. Spectrosc.*, 1998, 17, 41.
27. H. P. Boehm, *Carbon*, 1994, 32, 759.
28. J. L. Falconer, *Catal. Rev.-Sci. Eng.*, 1983, 25, 141.
29. J.L. Figueiredo, M.F.R. Pereira, M.M.A. Freitas, J.J.M. Órfao, *Carbon*, 1999, 37, 1379.
30. G. S. Szymanski, Z. Karpinski, S. Biniaka, A. Swiatkowski, *Carbon* 2002, 40, 2627.
31. Y. Nabae, K.D. Pointon and J.T.S. Irvine, *Energy Environ. Sci.*, 2008, 1, 148.
32. L. Zhang, J. Xiao, Y. Xie, Y. Tang, J. Liu and M. Liu, *J. Alloys Compd.*, 2014, 608, 272.
33. D. Cao, Y. Sun, Y. Xie and G. Wang, *J. Power Sources*, 2007, 167, 250.